J Membrane Biol (2013) 246:513–518
DOI 10.1007/s00232-013-9572-5

BRIEF COMMUNICATION

In Vivo Inhibition of Trans-Plasma Membrane Electron Transport by Antiviral Drugs in Grapevine

A. Panattoni · E. Rinaldelli · E. Triolo · A. Luvisi

Received: 28 November 2012 / Accepted: 1 June 2013 / Published online: 18 June 2013

Abstract Electrophysiological techniques were applied to investigate the action of antiviral drugs during trans-plasma events in in vivo grapevine cells infected by GLRaV-1 and GLRaV-3. Carbon fiber microelectrodes and redox-sensitive dyes were used to measure trans-plasma membrane electron transport (t-PMET) activity in healthy and infected samples treated with ribavirin, tiazofurin and oseltamivir. Each drug caused a reduction in oxidation current (expressed as $\Delta[Fe^{2+}]$) in healthy samples, indicating t-PMET inhibition. In almost all infected samples, the effect of drugs on t-PMET activity was significantly lower, suggesting that higher content of NADH in infected plants can interfere with t-PMET inhibition caused by drugs. Moreover, virus-infected samples exhibited elevated t-PMET activity compared to healthy samples. Analogous effects were observed by dye tests. Considering the effects of drugs on trans-plasma membrane potential, tests showed the activity of a proton pump during drug treatments with no significant difference with regard to health status.

Keywords Trans-plasma membrane electron transport · GLRaV-1 · GLRaV-3 · Ribavirin · Tiazofurin · Oseltamivir · Thioguanine

A. Panattoni · E. Triolo · A. Luvisi (✉)
Department of Agriculture, Food and Environment, University of Pisa, Via del Borghetto, 80, 56124 Pisa, Italy
e-mail: aluvisi@agr.unipi.it

E. Rinaldelli
Laboratory of Electrophysiology, Department of Crop, Soil and Environmental Science, University of Florence, sez. Arboriculture, Viale delle Idee, 30, 50019 Sesto Fiorentino, Florence, Italy

Introduction

Electrophysiological techniques can be applied to evaluate the effects of drugs in trans-plasma membrane events during their administration in animal or plant cells and tissues in vivo. The transport of solutes can be monitored by a trans-plasma membrane electric potential (t-PMEP) assay (Bush 1993; Rinaldelli et al. 2011), and transporters are involved in the uptake and efflux of chemical substances like drugs (Sherwood and Stollar 1984; Brandsch et al. 2008; Rubio-Aliaga and Daniel 2008; Wang and Wang 2009; International Transporter Consortium 2010). Trans-plasma membrane electron transport (t-PMET) is considered a target for developing antitumor drugs and allowing reduction of extracellular oxidants at the expense of cellular reducing equivalents that may derive from NADH or NADPH (Del Principe et al. 2011). This mechanism permits the t-PMET to maintain cellular redox homeostasis (Prata et al. 2010). In this way, cells can respond to changes in the redox microenvironment, regulating a variety of biological functions, including cell metabolism, proton pumping, activity of ion channels, growth and death (Ly and Lawen 2003).

With regard to chemotherapy in plants, t-PMEP of inosine monophosphate dehydrogenase (IMPDH) or purine biosynthesis inhibitors was electrophysiologically studied in grapevine explants infected by grapevine leafroll-associated virus 1 (GLRaV-1) (Luvisi et al. 2012), showing how drugs lead to biphasic electrical membrane response, suggesting an operation of H^+ cotransport. Moreover, in tobacco plants, the IMPDH inhibitor mycophenolic acid interferes with t-PMET activity linked to NAD^+/NADH conversion, acting differently in infected versus healthy samples during drug uptake by cells (Rinaldelli et al. 2012). Again, electrophysiological data can be supported

by a dye reduction assay using the cell-impermeable tetrazolium salt 2-(4-iodophenyl)-3-(4-nitrophenyl)-5-(2,4-disulfophenyl)-2H-tetrazolium monosodium salt (WST-1) (Berridge et al. 2005; Herst and Berridge 2007). In the presence of the intermediate electron acceptor 1-methoxy phenazine methylsulfate (PMS), WST-1 is reduced extracellularly to its soluble formazan via reducing equivalents derived from intracellular NADH (Prata et al. 2010).

Different chemotherapeutic strategies were performed for the eradication of GLRaV-1 and GLRaV-3 from plants (Panattoni et al. 2007; Skiada et al. 2009; Guta et al. 2010). IMPDH inhibitors (ribavirin [RB], tiazofurin [TZ]), a purine biosynthesis inhibitor (6-thioguanine [TG]) and a neuraminidase inhibitor (oseltamivir [OS]) eradicated both viruses at different rates, considering viral infection (Panattoni et al. 2011).

The aim of this study was to apply electrophysiological techniques to investigate the action of antiviral drugs belonging to three classes (De Clercq 2004) during transplasma events in in vivo cells infected by GLRaV-1 and GLRaV-3.

Materials and Methods

Plant Material

Field-grown *Vitis vinifera* cv. Sagrantino samples naturally infected by GLRaV-1 or GLRaV-3 were transferred to an insect-proof greenhouse. Seven-year-old plants, GLRaV-1 or GLRaV-3 single infection and virus-free (considering viruses included in European Commission directive 2005/43/EC), were used for t-PMET and t-PMEP trials. In June 2012, fully expanded leaves were excised and fresh freehand samples (3–5 mm) were cut with an ethanol-cleaned razor blade for testing (Rinaldelli et al. 2012).

For tissue culture, suspension cultured grape cells derived from grapevine cells were maintained in QL liquid medium (Quorin and Lepoivre 1977) containing 0.23 μM 2,4-D at 28 °C with shaking at 150 rpm on a gyrotary shaker and subcultured every 15 days with a 4 % inoculum (Yin et al. 2012).

Effect of Drugs on t-PMET

For the amperometric measurements, carbon fiber microelectrodes (CFMEs; tip diameter 5 μm) (Carbostar-1; Kation Scientific, Minneapolis, MN) were used following Rinaldelli et al. (2012). CFMEs were used in subsequent calibrations to test the linear response in the presence of the redox intermediary. Electrodes were placed in recording solution (RS) with a constant background of 5×10^{-4} M potassium ferricyanide ($K_3[Fe(CN)_6]$) (PF) (Table 1) adjusted to pH 5.6 by 2-(*N*-morpholino)ethanesulfonic acid (MES) and varying concentrations of potassium ferrocyanide ($K_4[Fe(CN)_6]$) (0, 20, 50, 100 μM). The oxidation current at an electrode potential of +400 mV was measured for each potassium ferrocyanide concentration.

The current at the CFME surface rises because the impermeant intermediary ferrocyanide, generated by the reduction of ferricyanide by cell reductase activity, is reoxidized by the CFME held at +400 mV. Calibration

Table 1 Solutions used in t-PMET and t-PMEP trials and parameters (cell reductase activity or membrane potential)

t-PMET trials			
Solution	Abbreviation	Cell reductase activity expressed as $[Fe^{2+}]$	Variation of cell reductase activity (%)
$MgSO_4$ 2×10^{-3} M, $CaSO_4$ 2×10^{-3} M, 5×10^{-4} $K_3[Fe(CN)_6]$	RS	$[Fe^{2+}]_{RS}$	
RS with RB at 0.60 mM	RB-RS	$[Fe^{2+}]_{RB}$	$[Fe^{2+}]_{RS}$–$[Fe^{2+}]_{RB} = \Delta[Fe^{2+}]_{RB}$
RS with TZ at 0.60 mM	TZ-RS	$[Fe^{2+}]_{TZ}$	$[Fe^{2+}]_{RS}$–$[Fe^{2+}]_{TZ} = \Delta[Fe^{2+}]_{TZ}$
RS with TG at 0.60 mM	TG-RS	$[Fe^{2+}]_{TG}$	$[Fe^{2+}]_{RS}$–$[Fe^{2+}]_{TG} = \Delta[Fe^{2+}]_{TG}$
RS with RB at 0.60 mM	OS-RS	$[Fe^{2+}]_{OS}$	$[Fe^{2+}]_{RS}$–$[Fe^{2+}]_{OS} = \Delta[Fe^{2+}]_{OS}$
t-PMEP trials			
Solution	Abbreviation	Membrane potential (Em)	Variation of membrane potential (%)
$CaSO_4$ 5.0×10^{-4} M, K_2SO_4 2.5×10^{-3} M, MES 5.0×10^{-3} M	BS	Em_{BS}	
BS with RB at 0.60 mM	RB-BS	$Em_{RB\text{-}BS}$	Em_{BS}–$Em_{RB\text{-}BS} = \Delta Em_{RB}$
BS with TZ at 0.60 mM	TZ-BS	$Em_{TZ\text{-}BS}$	Em_{BS}–$Em_{TZ\text{-}BS} = \Delta Em_{TZ}$
BS with TG at 0.60 mM	TG-BS	$Em_{TG\text{-}BS}$	Em_{BS}–$Em_{TG\text{-}BS} = \Delta Em_{TG}$
BS with RB at 0.60 mM	OS-BS	$Em_{OS\text{-}BS}$	Em_{BS}–$Em_{OS\text{-}BS} = \Delta Em_{OS}$

curves were used in order to estimate cell reductase activity, expressed as $[Fe^{2+}]$ using oxidation current values before each treatment (Rinaldelli et al. 2012). In order to evaluate the interference of drug with PF or CFME, 1-(2*R*,3*R*,4*S*,5*R*)-3,4-dihydroxy-5-(hydroxymethyl)oxolan-2-yl-1H-1,2,4-triazole-3-carboxamide (RB; Sigma-Aldrich, St. Louis, MO), (1*R*)-1-[4-(aminocarbonyl)-1,3-thiazol-2-yl]-1,4-anhydro-*D*-ribitol (TZ; kindly provided by Dr. Marquez, Center for Cancer Research, Frederick, MD), 2-amino-7H-purine-6-thiol (TG, Sigma-Aldrich) and ethyl(3*R*,4*R*,5*S*)-5-amino-4-acetamido-3-(pentan-3-yloxy)-cyclohex-1-ene-1-carboxylate) (OS; Roche Pharmaceuticals, Milan, Italy) at 0.60 mM were singularly added to solutions used for calibrations, comparing curves with the calibration ones.

Sample preparation and reductase activity detection were performed following Rinaldelli et al. (2012).

In order to stabilize the system before drug treatments, the leaf sample was maintained in RS until the oxidation current stabilized for at least 5 min. RS was then extracted using a syringe and renewed, measuring oxidation current until stabilization. The reductase activity difference between RS administrations ($\Delta[Fe^{2+}]_{RS}$, %) was calculated and repeated 15 times. Mean $\Delta[Fe^{2+}]_{RS} \pm \sigma$ was used as a threshold in order to establish system stability before each treatment. Drug treatments came before two sequential administrations of RS, with $\Delta[Fe^{2+}]_{RS}$ set within the threshold. Thus, RS was reextracted via syringe and substituted with drug-RS (Table 1). Oxidation current was measured until it stabilized for at least 5 min. $\Delta[Fe^{2+}]$ for each drug was calculated considering oxidation current after the last RS administration and oxidation current after drug administrations (Table 1).

All tests were conducted on 15 healthy or infected samples. Plots reported are representative of 15 equivalent experiments. Measurements were performed under a Faraday cage.

Redox-sensitive dye was used to confirm the CFME assay. tPMET activity was determined as described by Prata et al. (2010) using a microplate format. Cells (10^5/ml) were washed twice in 1-methoxy-5-methylphenazinium methylsulfate, resuspended in Hanks' balanced salt solution (HBSS) and incubated for 30 min at 37 °C with drugs dissolved in DMSO (<0.1 % final concentration) prior to adding WST-1/PMS solution (final concentrations 500 µM WST-1, 20 µM PMS). WST-1 reduction was determined after 20 min at 450 nm in a multiwell plate reader (Titertek Multiskan; Titertek Instruments, Huntsville, AL). All values were corrected for background readings of HBSS with drugs in the presence of WST-1/PMS. Effects of drugs were expressed as ΔA_{450} (ΔA_{450RB}, ΔA_{450TZ}, ΔA_{450OS}) between untreated and treated samples in each health status. Moreover, NADH was quantified in healthy and infected samples in a colorimetric assay (450 nm) using an NADH Quantification Kit (Sigma-Aldrich). All tests were conducted on 15 healthy or infected cell cultures.

Effect of Drugs on Trans-Plasma Membrane Potential

After preincubation for 1 h in basal solution (BS) (Table 1) adjusted to pH 5.6 with Tris (2-amino-2-hydroxymethyl-propane-1,3-diol), leaf segments were prepared according to Luvisi et al. (2012). Continuously aerated BS and drug-BS solutions (Table 1) were permitted to perfuse through the chamber at a flow rate of 10.0×10^{-3} l min^{-1}. The measuring electrodes used were micropipettes (tip diameter < 1 µm) obtained from single-barreled borosilicate capillaries (World Precision Instruments, Sarasota, FL) as described in Rinaldelli et al. (2012). Insertion of the microelectrodes took place in the central zone of the mesophyll by way of a micromanipulator. Treatments started after membrane potential (Em) stabilized for 5 min. Preincubation and electrophysiological tests were carried out at 22 °C (±0.5) under light (30 watt m^{-2}).

In order to confirm that drugs did not cause irreversible damage to the membrane at higher drug concentrations compared to those tested by Luvisi et al. (2012), repolarization of the membrane was investigated. Em after BS stabilization (Em_{BS}) and Em after drugs-BS stabilization ($Em_{drug\text{-}BS}$) (Table 1) were observed. Irreversible damage to the membrane was reported if stabilized $Em_{drug\text{-}BS}$ was significantly lower than Em_{BS}. The effect of drugs on membrane depolarization was calculated considering Em after BS stabilization and maximum Em achieved after drug-BS administration, expressed as ΔEm_{drug} (%).

In order to evaluate drug effects on Em, carbonyl cyanide *m*-chlorophenylhydrazone (CCCP), a protonophore and uncoupler of oxidative phosphorylation (Felle 1987; Marré et al. 1973) was used in 0.05 % ethanol, starting from a stock solution of 0.5 mM. Controls, in the different trials, also contained the same percentage of ethanol in the treatments. Moreover, treatments at low temperature (5 °C) were conducted following the same protocol of 22 °C (±0.5) tests. Sodium orthovanadate (Na_3VO_4) (Table 1), a relatively specific inhibitor of plasma membrane H^+-ATPase (Marré et al. 1989), was employed starting from a 5.0×10^{-3} M stock solution dissolving dry inhibitor in water and heating the solution for 3 h above 38 °C (O'Neill and Spanswick 1984). Controls in the trials also contained the same amount of Na (as Na_2SO_4) in the treatment.

All tests were conducted on 15 healthy or infected samples. Plots reported were representative of 15 equivalent experiments. Measurements were performed under a Faraday cage.

Statistical Analysis

The effects of treatments on $\Delta[Fe^{2+}]$, ΔEm, WST-1 reduction and influence on health status were elaborated using Sigma-Plot software (version 11; Systat Software, San Jose, CA). The software was used to perform two-way analysis of variance in a random design and pairwise multiple comparisons on significant effects and interactions using the Holm–Sidak method. Data expressed in percent were converted to arcsin values. $p < 0.05$ was considered to be significant.

Results and Discussion

CFME Response

The oxidation current response of the CFME was linear with respect to potassium ferrocyanide concentration (in a constant background of PF 5×10^{-4} M) in RS before each treatment, and no interference with RB, TZ and OS was observed. Conversely, TG interfered with the CFME. In the presence of TG, the oxidation current of the RS was set at 100–110 mV, precluding the measurement of interference of this drug against the cell reductase activity using CFME. The same oxidation current response was registered in the TG water solution, indicating that the CFME was able to oxidize the drug.

Effect of Health Status on t-PMET

Virus-infected samples exhibited elevated t-PMET activity compared to healthy samples. The $[Fe^{2+}]$ in healthy samples was set at 25.7 ± 3.6 μM, while GLRaV-1 and GLRaV-3 samples showed 33.9 ± 3.8 and 48.9 ± 8.5 μM $[Fe^{2+}]$, respectively. Analogous effects were observed by dye tests, where A_{450} was set at 0.234 ± 0.021 for healthy plants and at 0.301 ± 0.018 for GLRaV-1- and 0.315 ± 0.010 for GLRaV-3-infected cells. These data can be linked to the NADH content in GLRaV-1 and GLRaV-3 samples, which was set at 1.18 ± 0.05 and 1.22 ± 0.07 times higher than healthy samples, respectively.

$\Delta[Fe^{2+}]_{RS}$ in healthy samples was set at -3.7×10^{-3} %, and virus infection did not cause differences.

Effect of RB

Drug treatments that came before two sequential administrations of RS during which $\Delta[Fe^{2+}]_{RS}$ was set within the threshold caused a reduction in oxidation current (expressed as $\Delta[Fe^{2+}]_{drug}$) in healthy samples (Fig. 1), indicating t-PMET inhibition. Otherwise, the $\Delta[Fe^{2+}]_{RB}$ was significantly reduced in both infected samples (Table 2). Effects

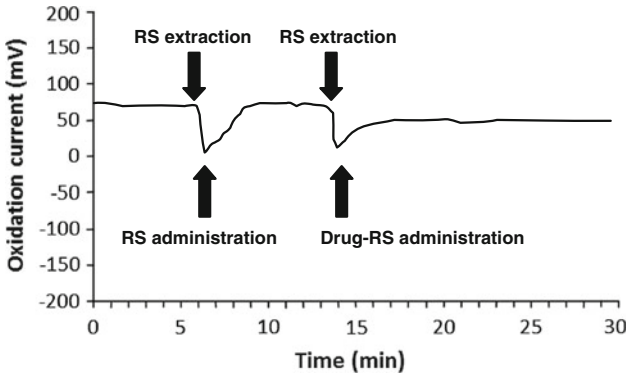

Fig. 1 Effect of ribavirin on oxidation current. Plot is representative of 15 equivalent experiments in healthy grapevine samples treated with ribavirin. *Arrows* The time of solution extraction or administration. *RS* recording solution, *Drug-RS* recording solution with drug at 0.60 mM

of RB on t-PMET were confirmed by dye reduction assay (Table 3). In healthy or infected samples, $Em_{RB\text{-}BS}$ was never lower than Em_{BS}, achieving 100 % of repolarization (Fig. 2). RB caused a membrane depolarization of 16.3 ± 1.5 % in healthy samples. Treatments with RB, performed in the presence of CCCP, did not provide any further effect on Em. Repolarization started, instead, after the inhibitor was removed. No significant difference with regard to health status was reported for RB. Treatments at low temperature (5 °C) completely eliminated the electrical response of the three drugs, with no differences according to health status. During sodium orthovanadate administration, the electrical response of the RS was completely eliminated in healthy and in infected samples (data not shown).

Effect of TZ

Similarly to RB treatment, TZ caused a reduction in oxidation current in healthy samples, indicating t-PMET inhibition. In both infected samples, $\Delta[Fe^{2+}]_{TZ}$ was significantly reduced (Table 2), even compared to RB (Table 3). Effects of TZ on t-PMET were confirmed by dye reduction assay (Table 3). $Em_{TZ\text{-}BS}$ was never lower than Em_{BS} as reported for RB, achieving 100 % of repolarization (Fig. 2). TZ caused a membrane depolarization of 17.1 ± 1.4 % in healthy samples. Em control tests (CCCP, low temperature and orthovanadate) showed the same results as for RB (data not shown).

Effect of OS

OS caused a reduction in oxidation current in healthy samples, more extensive than that of RB or TZ, indicating stronger t-PMET inhibition. In GLRaV-3-infected samples, $\Delta[Fe^{2+}]_{TZ}$ was significantly reduced (Table 2), while any

Table 2 Two-way factorial analysis of variance of $\Delta[Fe^{2+}]$ of *Vitis vinifera* cv. Sagrantino plants

Source of variation	df	SS	*p*
Treatment (A)	3	3.160	<0.001
Health status (B)	2	1.276	<0.001
A × B	6	1.402	<0.001
Residual	168	0.383	
Total	179	6.221	
Comparison for factor	DM	t	*p*
Comparison for B within RB-RS			
Healthy plant vs. GLRaV-1	0.100	5.760	<0.001
Healthy plant vs. GLRaV-3	0.0870	4.987	<0.001
GLRaV-1 vs. GLRaV-3	0.00135	0.774	NS
Comparison for B within TZ-RS			
Healthy plant vs. GLRaV-1	0.364	21.864	<0.001
Healthy plant vs. GLRaV-3	0.364	21.844	<0.001
GLRaV-1 vs. GLRaV-3	0.000333	0.0200	NS
Comparison for B within OS-RS			
Healthy plant vs. GLRaV-3	0.369	22.158	<0.001
GLRaV-1 vs. GLRaV-3	0.341	20.457	<0.001
Healthy plant vs. GLRaV-1	0.0283	1.701	NS

Healthy or GLRaV-1- or GLRaV-3-infected plants were treated with drug-RS. Pairwise multiple comparison analysis with the Holm–Sidak test was performed

RS recording solution, *Drug-RS* recording solution with drug at 0.60 mM, *RB* ribavirin, *TZ* tiazofurin, *OS* oseltamivir, *SS* sum of square, *df* degrees of freedom, *DM* difference of means, *t* t value, *NS* nonsignificant at $p > 0.05$

Table 3 t-PMET activity expressed as $\Delta[Fe^{2+}]$ using carbon fiber microelectrodes or as ΔA_{450} (%) using WST-1 assay

	$\Delta[Fe^{2+}]$ (%)		
	Healthy	GLRaV-1	GLRaV-3
RB	-35.0 ± 2.4^{a}*	-25.0 ± 2.2^{b}	-26.3 ± 3.4^{b}
OS	-44.2 ± 3.2^{a}	-43.0 ± 4.2^{a}	-10.1 ± 2.0^{b}
TZ	-36.7 ± 2.4^{a}	-3.3 ± 1.5^{b}	-3.7 ± 1.4^{b}
	ΔA_{450} (%)		
	Healthy	GLRaV-1	GLRaV-3
RB	-20.5 ± 2.2^{a}	-10.5 ± 1.2^{b}	-12.5 ± 1.0^{b}
OS	-26.6 ± 2.6^{a}	-25.0 ± 3.0^{a}	-9.6 ± 1.3^{b}
TZ	-21.2 ± 1.8^{a}	-2.1 ± 1.5^{b}	-2.2 ± 1.8^{b}

RB ribavirin, *TZ* tiazofurin, *OS* oseltamivir

* Values in the same column followed by the same letter do not differ significantly according to Duncan's multiple range test ($p = 0.05$)

variation was reported for GLRaV-1 samples compared to healthy ones (Table 3). Effects of OS on t-PMET were confirmed by dye reduction assay (Table 3). As with RB or TZ, the $Em_{OS\text{-}BS}$ was never lower than Em_{BS}, achieving 100 % of repolarization (Fig. 2). OS caused a membrane

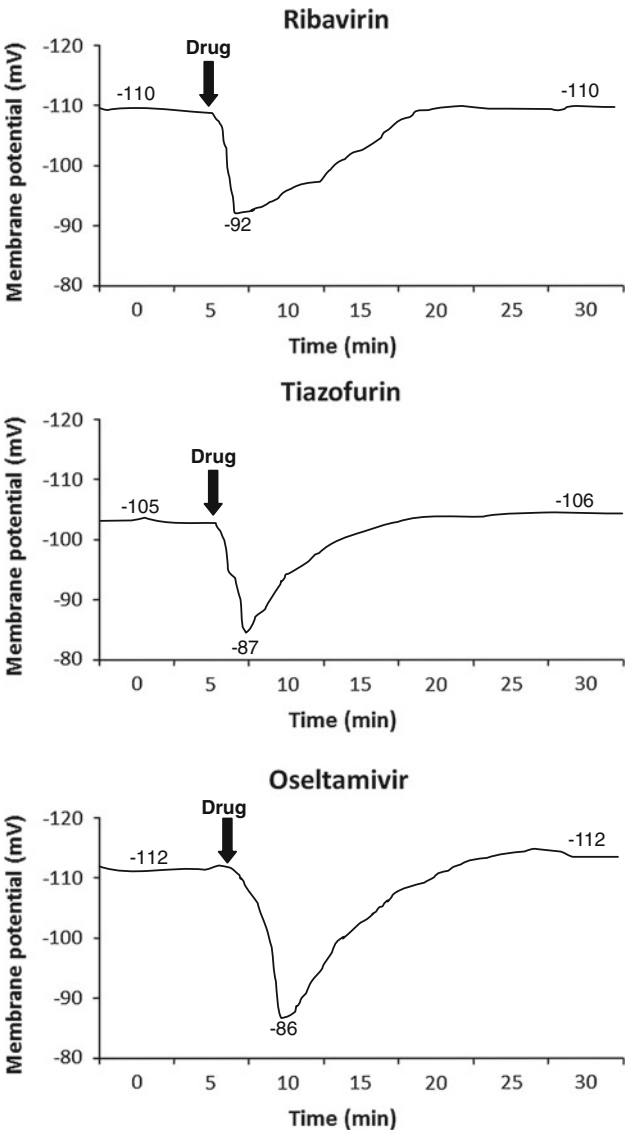

Fig. 2 Effects of drugs on membrane potential at 22 °C in healthy grapevine plants. *Plots* are representative of five equivalent experiments for each tested drug. *Arrows* The time of drug administration

depolarization of 23.4 ± 1.1 % in healthy samples. Em control tests (CCCP, low temperature and orthovanadate) showed the same results as for RB or TZ (data not shown).

In conclusion, the t-PMET activity in plants was reduced by all of the drugs. With regard to RB and TZ, their action as IMPDH inhibitors can interfere with NAD^{+}/NADH conversion, altering t-PMET activity. In the literature, the OS mechanism of action as an antiviral drug in plants has not been described, while its behavior in animal cells (Mendel et al. 1998; Sidwell et al. 1998) does not seem to carry over into the plant kingdom. To our knowledge, the inhibition of t-PMET activity by OS represents the first evidence of its interaction with plant cells.

In almost all infected samples, the effect of drugs on t-PMET activity was significantly lower, suggesting that a higher content of NADH in infected plants can interfere with t-PMET inhibition caused by drugs. Anyway, our findings showed that this interference of t-PMET inhibition varied according to drug. These results, as well as different eradication rates of viruses (Panattoni et al. 2011), indicate an as yet undescribed relationship between the mechanism of action of drugs and virus activity in plant cells.

The tested drugs did not cause ΔEm after CCCP treatment, suggesting that transport of RB, TZ and OS is metabolism-dependent. In fact, CCCP is an uncoupler of oxidative phosphorylation, which dissipates the electrochemical gradient of H^+ ions, preventing ATP synthesis. Consequently, active transport systems that require free energy to drive translocation (Bush 1993) are inhibited. Moreover, the tested drugs showed a strongly reduced membrane depolarization at low temperature, while treatments carried out under sodium orthovanadate, a specific inhibitor of H^+-ATPase, prove the activity of a proton pump during drug treatments. The health status of samples did not interfere with t-PMEP trials as reported for mycophenolic acid or purine biosynthesis inhibitors (Luvisi et al. 2012). Complete repolarization of membrane potential was achieved for RB, TZ and OS, indicating no irreversible damage to membranes due to drug administration.

References

Berridge MV, Herst PM, Tan AS (2005) Tetrazolium dyes as tools in cell biology: new insights into their cellular reduction. Biotechnol Annu Rev 1:127–152

Brandsch M, Knutter I, Bosse-Doenecke E (2008) Pharmaceutical and pharmacological importance of peptide transporters. J Pharm Pharmacol 60:543–585

Bush DR (1993) Proton-coupled sugar and amino acid transporters in plants. Annu Rev Plant Physiol Plant Mol Biol 44:513–542

De Clercq E (2004) Antivirals and antiviral strategies. Nat Rev Microbiol 2:704–720

Del Principe D, Avigliano L, Savini I, Catani MV (2011) Transplasma membrane electron transport in mammals: functional significance in health and disease. Antioxid Redox Signal 14:2289–2318

Felle H (1987) Proton transport and pH control in *Sinapis alba* root hairs: a study carried out with double-barrelled pH microelectrodes. J Exp Bot 38:340–354

Guta IC, Buciumeanu EC, Gheorghe RN, Teodorescu A (2010) Solutions to eliminate grapevine leafroll associated virus serotype 1 + 3 from *V. vinifera* L. cv. Ranai Magaraci. Rom Biotech Lett 15:72–78

Herst PM, Berridge MV (2007) Cell surface oxygen consumption: a major contributor to cellular oxygen consumption in glycolytic cancer cell lines. Biochim Biophys Acta 1767:170–177

International Transporter Consortium (2010) Membrane transporters in drug development. Nature 9:215–236

Luvisi A, Rinaldelli E, Panattoni A, Triolo E (2012) Membrane transport of antiviral drugs in plants: an electrophysiological study in grapevine explants infected by grapevine leafroll associated virus 1. Acta Physiol Plant 34(6):2115–2123

Ly JD, Lawen A (2003) Transplasma membrane electron transport: enzymes involved and biological function. Redox Rep 8:3–21

Marré E, Lado P, Rasi Caldogno F, Colombo R (1973) Correlation between cell enlargement in pea internode segments and decrease in the pH of the medium of incubation. II. Effects of inhibitors of respiration, oxidative phosphorylation and protein synthesis. Plant Sci Lett 1:185–192

Marré MT, Albergoni FG, Moroni A, Pugliarello MC (1989) Evidence that H^+ extrusion in *Elodea densa* leaves is mediated by an ATP-driven H^+ pump. Plant Sci 62:21–28

Mendel DB, Tai CY, Escarpe PA, Li W, Sidwell RW, Huffman JH, Sweet C, Jakeman KJ, Merson J, Lacy SA, Lew W, Williams MA, Zhang L, Chen MS, Bischofberger N, Kim CU (1998) Oral administration of a prodrug of the influenza virus neuraminidase inhibitor GS 4071 protects mice and ferrets against influenza infection. Antimicrob Agents Chemother 42(3):640–646

O'Neill SD, Spanswick RM (1984) Effects of vanadate on the plasma membrane ATPase of red beet and corn. Plant Physiol 75:586–591

Panattoni A, D'Anna F, Triolo E (2007) Antiviral activity of tiazofurin and mycophenolic acid against grapevine leafroll associated virus 3 in *Vitis vinifera* explants. Antivir Res 73:206–211

Panattoni A, Luvisi A, Triolo E (2011) Selective chemotherapy on grapevine leafroll-associated viruses. Phytoparasitica 39:503–508

Prata C, Grasso C, Loizzo S, Vieceli dalla Sega F, Caliceti C, Zambonin L, Fiorentini D, Hakim G, Berridge MV, Landi L (2010) Inhibition of trans-plasma membrane electron transport: a potential anti-leukemic strategy. Leuk Res 34:1630–1635

Quorin M, Lepoivre P (1977) Etude de millieux adaptes aux cultures in vitro de prunus. Acta Hortic 78:437–442

Rinaldelli E, Bandinelli R, Pagano M (2011) Short- and long-term effect of sulphite on sucrose transport in grapevine (*Vitis vinifera* L.), leaves. An electrophysiological study. Adv Hortic Sci 25(4): 245–252

Rinaldelli E, Panattoni A, Luvisi A, Triolo E (2012) Effect of mycophenolic acid on trans-plasma membrane electron transport and electric potential in virus-infected plant tissue. Plant Physiol Biochem 60:137–140

Rubio-Aliaga I, Daniel H (2008) Peptide transporters and their roles in physiological processes and drug disposition. Xenobiotica 38: 1022–1042

Sherwood A, Stollar V (1984) Evidence that ribavirin is transported in *Aedes albopictus* cells by the nucleoside transport system. Antivir Res 4(6):317–324

Sidwell RW, Huffman JH, Barnard DL, Bailey KW, Wong MH, Morrison A, Syndergaard T, Kim CU (1998) Inhibition of influenza virus infections in mice by GS4104, an orally effective influenza virus neuraminidase inhibitor. Antivir Res 37(2): 107–120

Skiada FG, Grigoriadou K, Maliogka VI, Katis NI, Eleftheriou EP (2009) Elimination of grapevine leafroll-associated virus 1 and grapevine rupestris stem pitting-associated virus from grapevine cv. Agiorgitiko, and a micropropagation protocol for mass production of virus-free plantlets. J Plant Pathol 91:177–184

Wang HP, Wang CL (2009) Biological transporters as targets for new drugs design. J Exp Clin Med 1:31–38

Yin Y, Borges G, Sakuta M, Crozier A, Ashihara H (2012) Effect of phosphate deficiency on the content and biosynthesis of anthocyanins and the expression of related genes in suspension-cultured grape (*Vitis* sp.) cells. Plant Physiol Biochem 55:77–84